International Journal of Computing and Digital Systems
ISSN (2210-142X)
Int. J. Com. Dig. Sys. 14, No.1 (Sep-2023)

http://dx.doi.org/10.12785/ijcds/140177

Improved Classification of Medical Histopathological Images with Fusion of Thepade SBTC and Bernsen Thresholding using Machine Learning

Sudeep D. Thepade[1] **and Ayush G. Dudhani**[2]

[1]*Computer Engineering Dept., Pimpri Chinchwad college of Engineering, Pune, India*
[2]*Computer Engineering Dept., Pimpri Chinchwad college of Engineering, Pune, India*

Received 06 Apr. 2023, Revised 03 Jun. 2023, Accepted 31 Jul. 2023, Published 01 Sep. 2023

Abstract: Histopathological images play an important role in selecting effective therapies; they are necessary for determining the health of a particular biological structure and diagnosing disorders like cancer. Machine learning for medical diagnosis reduces the likelihood of a misdiagnosis. Efficiency gains are the main benefit of applying machine learning (ML) to medical diagnosis. ML gives the medical community more time to concentrate on their profession as Artificial Intelligence improves. Investigating the classification performance of several ML Algorithms might be fascinating. On datasets, these algorithms are first trained. Machine learning algorithms are trained using many custom features. To improve cancer detection through the classification of histopathological images, the work the paper demonstrates the Thepade SBTC (Sorted Block Truncation Coding) global features and their fusion with Bernsen Thresholding extracted local features. Utilizing the 960 images from the KIMIA Path960 Dataset [1], experimental validation is carried out with performance indicators alias specificity, sensitivity, and accuracy. Here the feature fusion of Thepade SBTC and Bernsen binarization has shown improved classification of histopathological images over consideration of individual features. The ensemble of ML algorithms with majority voting logic has improved the classification of histopathological images over individual ML algorithms. The Ensemble of 'LMT, Simple Logistic (SL), and Multilayer Perceptron (MP)' for TSBTC 9-ary and fusion with Bernsen binarization feature give the same accuracy of 97.3958% in a ten-fold cross-validation scenario as the Ensemble of 'Simple Logistic, Multilayer Perceptron, and Random Forest (RF)' for TSBTC 9-ary and fusion with Bernsen binarization feature.

Keywords: Histopathological images, Image processing, machine learning, Bernsen thresholding, Thepade SBTC

1. INTRODUCTION

About 10 million and above deaths (approximately about one in six deaths) were caused due to cancer growth in 2020, creating it the top cause of death globally [2]. The most prevalent types of cancer are Lung, Colon, Rectum, and prostate cancer. Early discovery and handling of cancer cases reduce death. Early detection of cancer increases the probability that it will react to treatment, increasing the probability of survival with less illness and requiring less expensive treatment. Early cancer detection and avoiding care delays can significantly enhance the lives of cancer patients.

The study of an organism's cells and tissues at a microscopic level by a histopathologist is covered by the important biological field of histopathology. Histopathological images [3] play a significant role in selecting effective therapies; they can be helpful for the diagnosis of disorders like cancer as well. Digital histopathology is a key advancement in contemporary medicine. There are surprisingly few skilled medical professionals. ML is important in making an initial diagnosis when there are few qualified practitioners. The classification of histopathology images [4] for cancer diagnosis uses traditional ML algorithms.

The objective of this study was to enhance the precision of categorizing histopathological images by utilizing multiple ML algorithms as well as their combination. Thepade SBTC [5] is used to get local features. Fusion of these features with global Bernsen thresholding [6] features has been experimented with. There are several feature extraction techniques in the literature. Algorithms and classifiers for machine learning are trained using the extracted features.

The following constitutes the work's primary contributions:

- Improved Classification of Histopathological Images by feature fusion of Bernsen Thresholding and Thepade SBTC [7] for variations of TSBTC N-ary.

E-mail address: sudeepthepade@gmail.com, dudhaniayush@gmail.com

- Ensemble of ML algorithms to improvise Histopathological Image Classification.
- The KIMIAPath960 dataset of histopathological images is examined using a proposed method, and performance metrics alias accuracy, sensitivity, and specificity are utilized to assess its effectiveness.

The paper is drafted with the following sections. There is a review of existing work in Section 2. Section 3 has a proposed approach for categorizing histopathological images. In Section 4, the outcomes of the suggested technique are examined. Section 5 discusses the Key Observations, while Section 6 contains the conclusion.

2. LITERATURE SURVEY

For categorizing histopathology images for cancer detection, the bulk of studies has experimented with several ML Algorithms with various image content descriptions. The main advancements in categorizing histopathology images to date may be divided into two categories: developing the architecture of deep convolutional neural networks (CNN) and utilizing the appropriate machine learning methods to extract attributes representing image content.

One major benefit of deep learning [8] is that feature extraction can be accomplished indirectly without requiring explicit manual feature engineering. However, this approach is also characterized by limitations, such as the lengthy training time and the need for considerable training data.

SVM, Artificial Neural Networks, and Decision Trees were used by the authors of Alhindi et al. [9] to take into account several features, including Local Binary Pattern (LBP), Histogram of Oriented Gradients (HOG), and a pre-trained deep network. This study's SVM attains the highest accuracy of 90.52

Authors have identified land usage from aerial photographs in Thepade et al. [5]. They have combined a variety of machine learning algorithms. The merging of SBTC and Savoula thresholding techniques is also considered for greater precision.

Authors Anurag et al. [10] developed a feature blending strategy for effective histopathological image categorization for cancer detection. The pre-trained architecture for CNN-based feature extraction is referred to as MobileNetV2.

In their study, Senan et al. [11] employed the CNN method (specifically, AlexNet) to extract highly detailed features from the BreakHis dataset and classify its images. This approach yielded impressive results with accuracy, specificity, AUC, and sensitivity values of 95

Alexander et al. [12] utilized CNN for image classification of a histopathological dataset of breast cancer. They have used the microscopic histopathological stained images presented in the ICIAR 2018 Grand Challenge. The approach they have utilized makes use of neural networks along with gradient-boosted trees for classification. Their results for 2-class and 4-class classification were 93.8

In [13], S. D. Thepade et al. evaluates the use of pre-trained DCNN models and their integration with Thepade SBTC 10-ary features to enhance the accuracy of ML classifiers [14] for human face presentation threat detection, which is a crucial area of research in contact-free identification. These results indicate that this approach can enhance the performance of Face Presentation Attack Detection systems.

The authors of [15] employed an ensemble of ML algorithms to classify polarimetric SAR data, achieving superior results compared to individual algorithms in isolation.

While the traits are generally derived from global or local perception, it is essential to look into how the two perceptions interact. Additionally, while individual machine learning classifiers are used to categorize histopathology images, utilizing ensembles of different machine learning techniques yields more exciting results.

3. PROPOSED SYSTEM

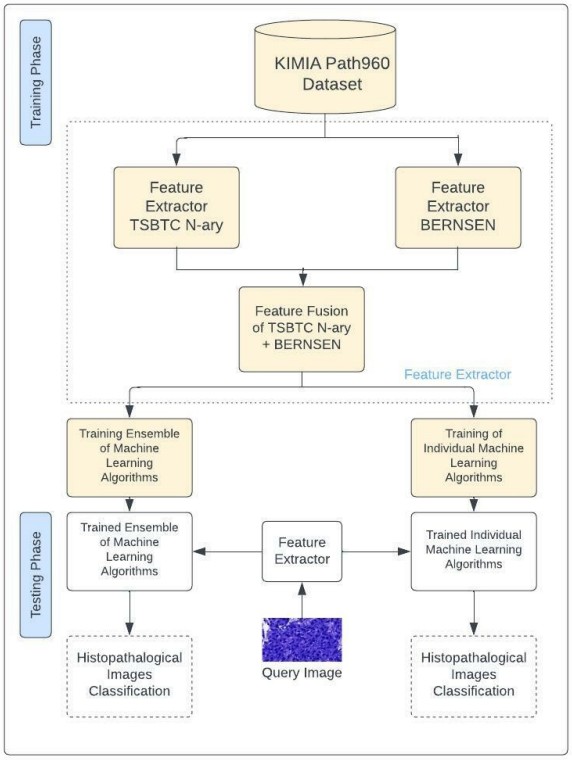

Figure 1. Block diagram showing the two steps: training and testing of the proposed classification model

As elucidated in Figure 1, the methodology proposed for classifying histopathological images has two phases: training and testing. The ML algorithms are trained on features

obtained from the KIMIA Path960 dataset's histopathological images in the training. The feature extraction unit uses Bernsen thresholding logic and Thepade SBTC N-ary to extract features from each image. The merging of Thepade SBTC and Bernsen features is denoted as "BERNSEN + TSBTC N-ary feature fusion". During the training phase, individual ML classifiers and ensembles were employed, leveraging the characteristics of the histopathological images.

The feature extraction module receives a query histopathology image in the testing phase. The pre-trained ML algorithms, or a group of ML algorithms, categorize the image based on features obtained from the query histopathology image.

Thepade SBTC N-ary, used for global feature extraction, and Bernsen thresholding, used for local feature extraction, are discussed in greater detail in subsections A and B. The suggested feature-level fusion [16] and an ensemble of ML algorithms with the logic of majority voting are explained in detail in subsections C and D, respectively.

A. *Thepade Sorted Block Truncation Code (Thepade SBTC)*

Suppose 'I' represent an image with dimensions 'a x b' and comprises three colour planes: R, B, and G. The feature vectors of TSBTC N-ary, which consist of i-th group average of each colour plane devised with TSBTC N-ary, can be expressed as [TSBR1, TSBR2,..., TSBRn, TSBG1, TSBG2,..., TSBGn, TSBB1, TSBB2, ..., TSBBn], where TSBRk, TSBGk, and TSBBk represent the k-th group centroids of each colour plane.

For Thepade SBTC-2 ary, an image I composed of 'a x b' pixels with RGB colour planes is converted into a single-dimensional vector and arranged as sort_R, sort_G, and sort_B. The Thepade SBTC-2ary feature array is calculated as [TSBR1, TSBR2, TSBG1, TSBG2, TSBB1, TSBB2] as shown in equations:

$$TSBR1 = \frac{2}{ab} \sum_{z=1}^{\frac{ab}{2}} sort\_R(z) \quad (1)$$

$$TSBR2 = \frac{2}{ab} \sum_{z=1}^{\frac{ab}{2}} sort\_R(z) \quad (2)$$

$$TSBG1 = \frac{2}{ab} \sum_{z=1}^{\frac{ab}{2}} sort\_G(z) \quad (3)$$

$$TSBG2 = \frac{2}{ab} \sum_{z=1}^{\frac{ab}{2}} sort\_G(z) \quad (4)$$

$$TSBB1 = \frac{2}{ab} \sum_{z=1}^{\frac{ab}{2}} sort\_B(z) \quad (5)$$

$$TSBB2 = \frac{2}{ab} \sum_{z=1}^{\frac{ab}{2}} sort\_B(z) \quad (6)$$

In the proposed histopathological image classification, nine different TSBTC [17] [18] [19] versions have been tested, from TSBTC 2 to 10 ary.

B. *BERNSEN Thresholding*

Bernsen's locally adaptive binarization technique [20] is frequently employed for feature extraction from grayscale images. This method has been tested with various neighbourhood values and contrast limitations. The threshold for this technique is determined by taking the average of the minimum and maximum intensity values in a w×w neighbourhood. These values are denoted as minN and maxN, respectively.

$$t = \frac{minN+maxN}{2} \quad (7)$$

However, the threshold is only used if the local contrast exceeds a predefined limit, cmin. Local contrast is defined as the intensity range in the neighbourhood and is denoted as lc.

$$lc = maxN - minN \quad (8)$$

If lc is less than the contrast limit, c, then the pixel is assumed to belong to the background class and is not considered for feature extraction.

C. *Histopathological Image Feature Fusion of Thepade SBTC and Bernsen Thresholding*

One approach for histopathology image classification involves combining the TSBTC N-ary and Bernsen thresholding techniques to achieve feature-level fusion [21], which involves applying both techniques to the RGB colour planes of the image 'I', resulting in a set of thresholded images. The feature vector for the fusion of these techniques can then be represented as a concatenation of the features extracted from each thresholded image, denoted as TSBR1, TSBR2, TSBRn, TSBG1, TSBG2, ..., TSBGn, TSBB1, TSBB2, ..., TSBBn, BR1, BR2, BG1, BG2, BB1, and BB2.

D. *Ensemble of ML Algorithms*

Here, the ensemble of several algorithms [22] with the concept of majority voting is used to consider the ML algorithms from the families of Bayes, functions, lazy, and trees.

The following classifiers are considered:

- From Bayes family: Bayes Net and Naïve Bayes
- Functions family: SMO, SL and MP
- Lazy: IBk and KStar
- Trees: J48, RF, REPTree, Random Tree and LMT

They are tried here in the proposed categorization method of Histopathological images. The investigation of an ensemble of SL, RF, LMT, and MP with the logic of majority voting is done as these were the best-performing classifiers.

4. RESULTS AND DISCUSSION

With the aid of the Weka tool, experiments are conducted in Python for the proposed classification of the

histological images. Different Python libraries like OpenCV, Doxapy, Numpy and Pandas are used. For testing, the KIMIA Path960 dataset is used. Twenty different groups of tissues are represented by a total of 960 images in the dataset (48x20). Figure 2 displays several histopathology examples for each of these groups.

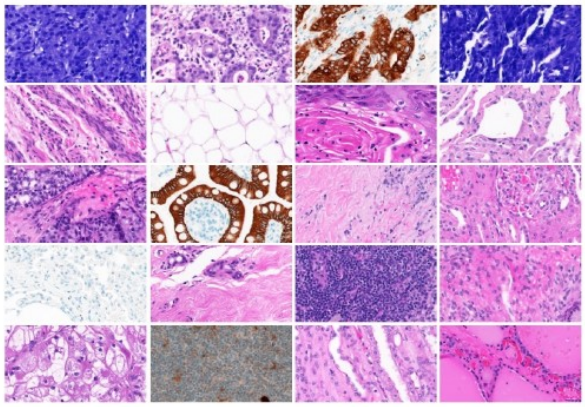

Figure 2. KIMIA Path960 image dataset samples for 20 classes

The performance analysis of all types of methods of histopathological image classification is done using the percentage accuracy of classification, Sensitivity, and Specificity, which can be computed as given in the equation.

$$Accuracy = \frac{Tp+Tn}{Tp+Tn+Fp+Fn} \quad (9)$$

$$Sensitivity = \frac{Tp}{Tp+Fn} \quad (10)$$

$$Specificity = \frac{Tn}{Tn+Fp} \quad (11)$$

Where,

Tp = True Positive = An outcome when the image class is accurately identified.

Tn = True Negative = The outcome when the image class is incorrectly detected.

Fp = False Positive = A conclusion reached when the algorithm correctly recognizes an image as not of the class under consideration.

Fn = False Negative = a type of error in which a test or classification algorithm fails to identify a true positive instance, meaning it indicates that something is absent when it is present.

Thepade Sorted Block Truncation Code

The proposed categorization of histopathological images was tested using the KIMIA Path960 dataset, with 399 variants employing 12 ML classifiers and nine ensembles, nine variants of TSBTC N-ary feature, Bernsen thresholding feature, and nine variants of feature combination of TSBTC and Bernsen.

TSBTC 2-ary to 10-ary and Bernsen features are tested initially on 12 different ML algorithms. As shown in Figure 3, the initial % improvement from TSBTC 2-ary to 7-ary is extremely impressive. The improvement in accuracy from TSBTC 7-ary to 10-ary is merely minimal. After testing TSBTC N-ary on various classifiers, the best accuracy is shown by TSBTC 9-ary refer Table I.

It is observed from Figure 3 that the best-performing classifiers are LMT, SL, MP, RF and KStar. So, the ensemble of these five classifiers with different combinations is considered.

Considering TSBTC N-ary up to 10-ary and applying the best-performing machine learning algorithms like SL + MP + LMT + RF, SP + MP + KStar + RF, SL + MP +RF, SL + MP, SL + RF, MP + RF, LMT + SL, LMT + MP + SL and LMT + MP Under 10-fold cross-validation, majority voting gave better performance than applying individual algorithms.

Figure 4 shows the graph when a combination of ML algorithms is applied for Bernsen local features and TSBTC N-ary local features. Again TSBTC 7-ary to 10-ary gives better performance.

Table II and Figure 4 show that an ensemble of four ML algorithms (SL + MP + RF + LMT) performs better with 97.29% accuracy. Further fusion has been experimented which resulted in better accuracy.

Now combination of TSBTC N-ary with Bernsen features is extracted and tested against individual ML classifiers, as shown in Figure 5. The top ML classifiers here are the same indicated in Table III.

The highest accuracy observed is 97.19% for TSBTC 9-ary fusion with Bernsen against SL and LMT classifiers. TSBTC 7-ary fusion with Bernsen features against LMT classifier. Further testing against the fusion of top-performing classifiers gives better performance.

Figure 6 displays the accuracy obtained after comparing the combination of global and local features with the combination of ML classifiers. The highest accuracy of 97.40% is achieved at two places. Figure 6 shows that the fusion of TSBTC 9-ary and Bernsen features gives maximum accuracy for an ensemble of three ML algorithms for SL + MP + RF and for an ensemble of LMT + MP + SL which is 97.3958% (97.40%) accuracy.

Other performance matrix Sensitivity and Specificity also gave the same values for both the ensembles shown in Table IV. Thus, both are considered for the best results.

TABLE I. TOP PERFORMING TSBTC VARIANTS AGAINST ML CLASSIFIER

	TSBTC 7-ary	TSBTC 8-ary	TSBTC 9-ary	TSBTC 10-ary
Simple Logistic	96.67%	96.56%	96.67%	96.04%
Multilayer Perceptron	95.31%	95.21%	95.94%	96.35%
KStar	94.38%	94.27%	94.27%	94.48%
Random Forest	94.27%	94.48%	95.79%	94.48%
LMT	97.29%	96.56%	96.88%	96.67%

TABLE II. TSBTC 7-ARY TO 10-ARY TESTED AGAINST THE COMBINATION OF ML ALGORITHMS

	TSBTC 7-ary	TSBTC 8-ary	TSBTC 9-ary	TSBTC 10-ary
SL + MP + KStar + RF	97.08%	96.88%	96.77%	96.77%
SL + MP + RF	96.88%	96.67%	97.08%	96.98%
SL + MP	96.56%	96.98%	96.88%	96.35%
SL + RF	97.08%	96.98%	96.98%	96.25%
MP + RF	95.94%	95.52%	95.83%	96.56%
LMT + SL	97.08%	96.56%	96.88%	96.46%
LMT + MP + SL	97.19%	96.98%	96.88%	96.67%
LMT + MP	97.19%	96.98%	96.88%	96.88%
SL + MP + RF + LMT	**97.29%**	97.08%	97.08%	96.98%

TABLE III. GLOBAL AND LOCAL FEATURES FUSION TESTED AGAINST INDIVIDUAL ML CLASSIFIERS

	TSBTC 10-ary + Bernsen	TSBTC 9-ary + Bernsen	TSBTC 8-ary + Bernsen	TSBTC 7-ary + Bernsen
SL	96.56%	**97.19%**	96.56%	97.08%
MP	95.73%	95.73%	95.63%	95.31%
KStar	94.27%	94.48%	94.79%	94.48%
RF	94.58%	94.48%	94.58%	94.79%
LMT	96.67%	**97.19%**	96.67%	**97.19%**

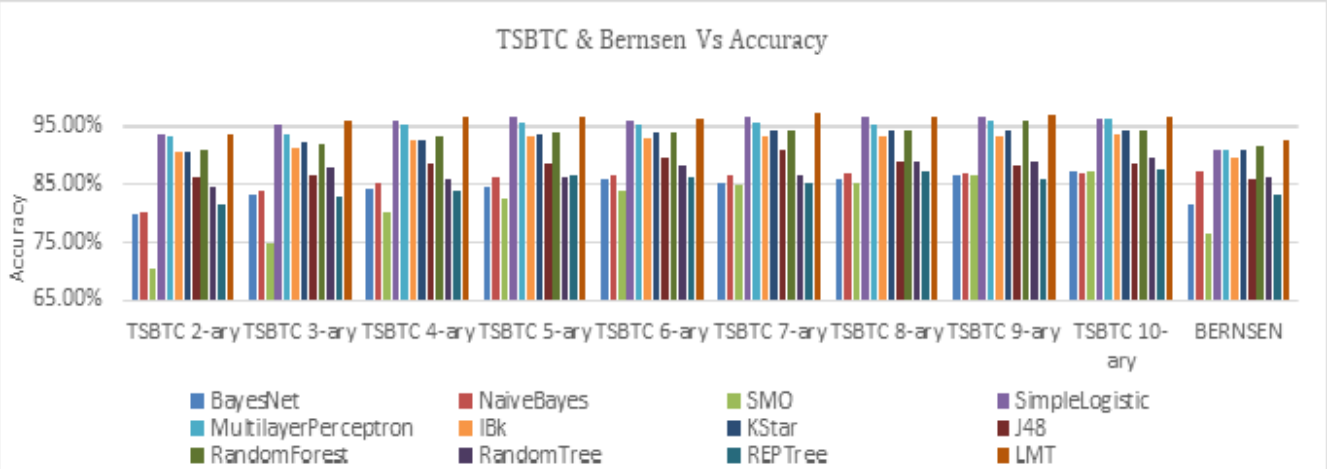

Figure 3. Accuracy based performance of ML algorithms in histopathological image categorization for respective features like TSBTC N-ary & Bernsen features

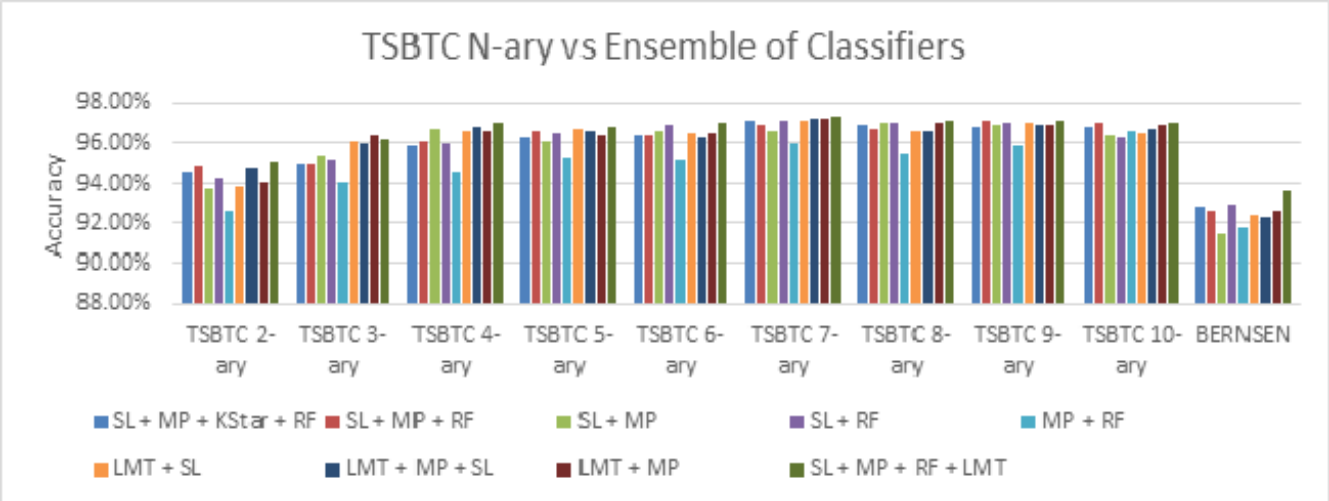

Figure 4. Accuracy based performance of ML Ensembles in histopathological image categorization for respective features as TSBTC N-ary& Bernsen features

TABLE IV. PERFORMANCE METRICS OF 9-ARY TSBTC + BERNSEN USING AN ENSEMBLE OF ML ALGORITHMS

9-ary + Bernsen	Accuracy	Sensitivity	Specificity
Simple Logistic + Multilayer Perceptron + Random Forest	97.40%	0.974%	0.999%
Simple Logistic + Multilayer Perceptron + LMT	97.40%	0.974%	0.999%

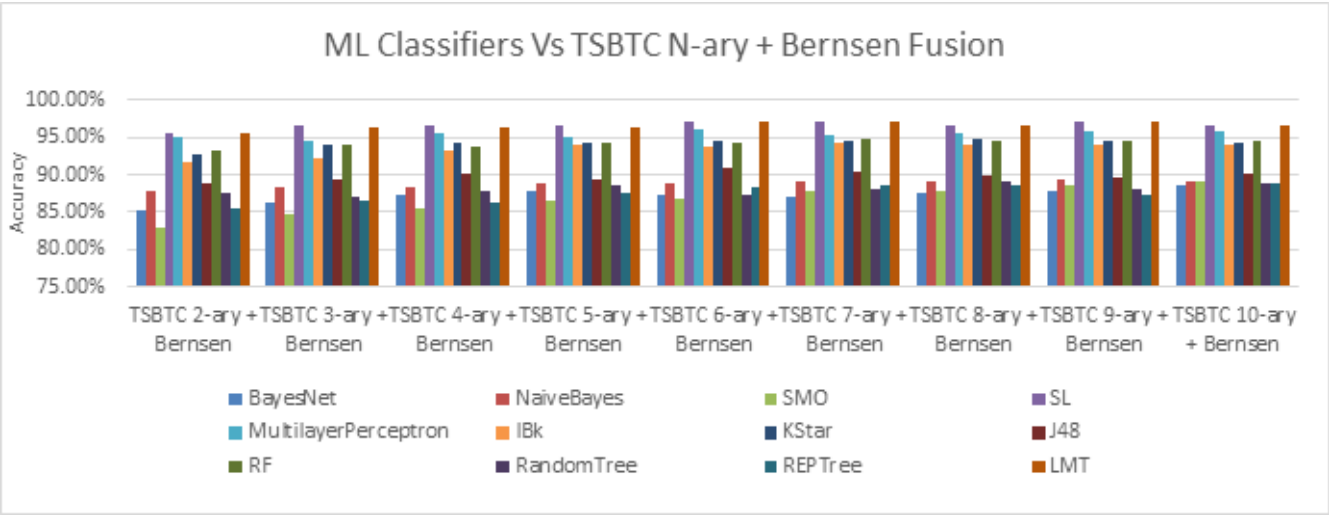

Figure 5. Accuracy based performance of ML algorithmses in histopathological image categorization for proposed feature fusion 'TSBTC N-ary + Bernsen'

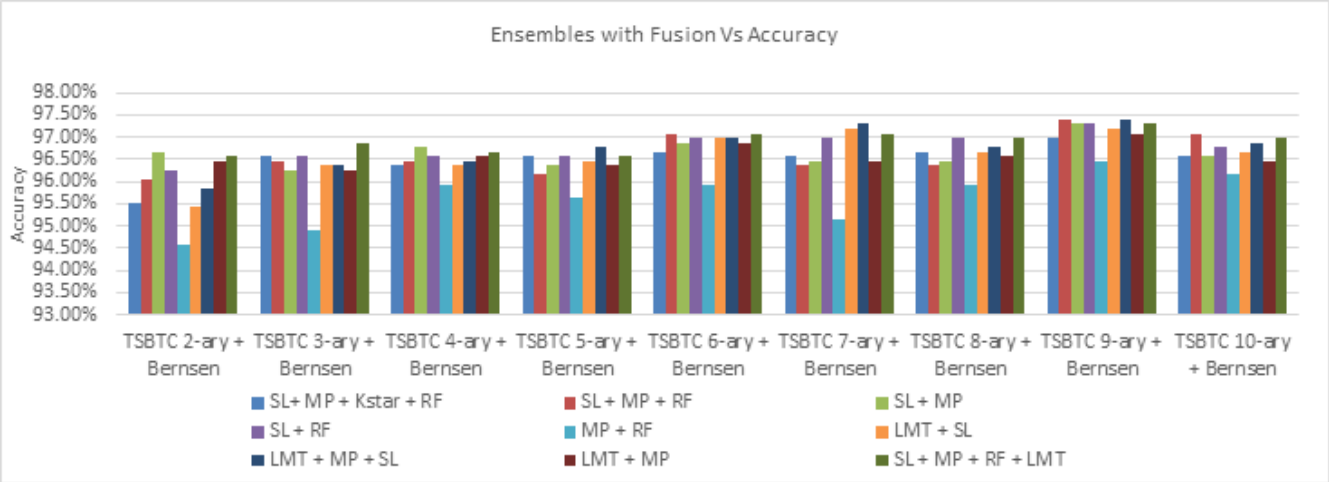

Figure 6. Accuracy based performance of ML Ensembles in histopathological image categorization for proposed feature fusion 'TSBTC N-ary + Bernsen'

TABLE V. PERFORMANCE EVALUATION OF THE PROPOSED METHOD WITH RELEVANT EXISTING METHODS OF HISTOPATHOLOGICAL IMAGE CLASSIFICATION FOR THE KIMIA PATH 960 DATASET

Authors	Dataset used	Technique used	Performance Metrics	
Ambarish et al. [8]	KIMIA Path960	Custom ResNet50 + AdamW	Accuracy	99.90%
		Custom ResNet50 + Adam	Accuracy	99.77%
		Custom ResNet50 + AdaMax	Accuracy	99.79%
		Custom ResNet50 + Radam	Accuracy	99.27%
Meghna et al. [1]	KIMIA Path960	Deep features	Accuracy	94.72%
		LBP	Accuracy	90.62%
		BoVW	Accuracy	96.50%
Alhindi et al. [9]	KIMIA Path960	SVM + features from LBP	Accuracy	90.52%
		SVM + deep features	Accuracy	81.14%
		ANN + HOG	Accuracy	34.37%
Anurag et al. [10]	KIMIA Path960	NN + GLCM + average of ordered grey values (Feature size 1x20)	AUC	0.999
			F1 score	0.951
			Precision	0.951
			Recall	0.951
		RF + GLCM + average of ordered grey values (Feature size 1x20)	AUC	0.999
			F1 score	0.951
			Precision	0.951
			Recall	0.951
		SVM + GLCM + average of ordered grey values (Feature size 1x20)	AUC	0.999
			F1 score	0.951
			Precision	0.951
			Recall	0.951
Proposed Method	KIMIA Path960	Ensemble of (RF + SL + MP) or (SL + MP + LMT) + TSBTC 9-ary features and Bernsen features	Accuracy	97.40%
			Sensitivity	0.974
			Specificity	0.999

5. DISCUSSION AND OBSERVATIONS

The TSBTC N-ary method was used to extract global features in this study, with TSBTC 7-ary exhibiting superior performance compared to other N-ary values. Furthermore, the combination of TSBTC N-ary and Bernsen features resulted in better performance than using either TSBTC N-ary or Bernsen features alone.

The findings of our study indicate that the optimal performance was achieved through an ensemble of machine learning classifiers utilizing a combination of TSBTC 9-ary and Bernsen features. More precisely, a combination of TSBTC 9-ary and Bernsen thresholding, along with the ensembles "SL + RF + MP" and "LMT + MP + SL", resulted in an accuracy of 97.3958%, a sensitivity of 0.974, and a specificity of 0.999. Table V compares the proposed method with the existing methods.

6. CONCLUSION AND FUTURE SCOPE

In 2020, one in six deaths, or around 10 million deaths, are because of cancer, making it the highest cause of death globally. The most common forms of cancer include breast, lung, colon, rectum, and prostate. When cases are identified and treated, cancer mortality is decreased.

ML can play a major role in preliminary diagnosis with fewer expert practitioners. Conventional ML Algorithms are used to classify histopathological images for cancer detection.

Histopathological images play a significant role in selecting effective therapies; they are necessary for determining the health of a particular biological structure and diagnosing disorders like cancer.

Thepade SBTC 9-ary and Bernsen thresholding features combined with an ensemble of "RF, SL and MP" or "SL, MP and LMT" gave the best overall performance.

Experimentation is performed on so many images that the best performance is observed by feature fusion with the ensemble.

Furthermore, observing the combination of multiple features derived using various techniques from histopathology images for cancer detection would be intriguing.

REFERENCES

[1] M. Dinesh Kumar, M. Babaie, S. Zhu, S. Kalra, and H. R. Tizhoosh, "A comparative study of cnn, bovw and lbp for classification of histopathological images," in *2017 IEEE Symposium Series on Computational Intelligence (SSCI)*, 2017, pp. 1–7.

[2] WHO, "Cancer," *WHO Newsroom*, 2022. [Online]. Available: https://www.who.int/news-room/fact-sheets/detail/cancer

[3] S. M. Ayyad, M. Shehata, A. Shalaby, M. Abou El-Ghar, M. Ghazal, M. El-Melegy, N. B. Abdel-Hamid, L. M. Labib, H. A. Ali, and A. El-Baz, "Role of ai and histopathological images in detecting prostate cancer: A survey," *Sensors*, vol. 21, no. 8, p. 2586, Apr 2021. [Online]. Available: http://dx.doi.org/10.3390/s21082586

[4] A. Belsare and M. Mushrif, "Histopathological image analysis using image processing techniques: An overview," *Signal Image Process Int J*, vol. 3, 11 2011.

[5] S. D. Thepade and P. R. Chaudhari, "Land usage identification with fusion of thepade sbtc and sauvola thresholding features of aerial images using ensemble of machine learning algorithms," *Applied Artificial Intelligence*, vol. 35, no. 2, pp. 154–170, 2021. [Online]. Available: https://doi.org/10.1080/08839514.2020.1842627

[6] J. Bernsen, "Dynamic thresholding of grey-level images,[in:] proc. of the 8th int," in *Conf. on Pattern Recognition*, 1986.

[7] S. R. Badre and S. D. Thepade, "Novel video content summarization using thepade's sorted n-ary block truncation coding," *Procedia Computer Science*, vol. 79, pp. 474–482, 2016, proceedings of International Conference on Communication, Computing and Virtualization (ICCCV) 2016. [Online]. Available: https://www.sciencedirect.com/science/article/pii/S1877050916001927

[8] A. Ganguly, R. Das, and S. K. Setua, "Histopathological image and lymphoma image classification using customized deep learning models and different optimization algorithms," in *2020 11th International Conference on Computing, Communication and Networking Technologies (ICCCNT)*, 2020, pp. 1–7.

[9] T. J. Alhindi, S. Kalra, K. H. Ng, A. Afrin, and H. R. Tizhoosh, "Comparing lbp, hog and deep features for classification of histopathology images," in *2018 International Joint Conference on Neural Networks (IJCNN)*, 2018, pp. 1–7.

[10] A. Anurag, R. Das, G. K. Jha, S. D. Thepade, N. DSouza, and C. Singh, "Feature blending approach for efficient categorization of histopathological images for cancer detection," in *2021 IEEE Pune Section International Conference (PuneCon)*, 2021, pp. 1–6.

[11] E. Senan, F. Alsaade, M. Ibrahim, A. Al-Mashhadani, T. Aldhyani, and M. Al-Adhaileh, "Classification of histopathological images for early detection of breast cancer using deep learning," *Journal of Applied Science and Engineering (Taiwan)*, vol. 24, pp. 323–329, 01 2021.

[12] A. Rakhlin, A. Shvets, V. Iglovikov, and A. A. Kalinin, "Deep convolutional neural networks for breast cancer histology image analysis," in *Image Analysis and Recognition*, A. Campilho, F. Karray, and B. ter Haar Romeny, Eds. Cham: Springer International Publishing, 2018, pp. 737–744.

[13] S. D. Thepade, M. R. Dindorkar, P. R. Chaudhari, and S. V. Bang, "Enhanced face presentation attack prevention employing feature fusion of pre-trained deep convolutional neural network model and thepade's sorted block truncation coding," *International Journal of Engineering*, vol. 36, no. 4, pp. 807–816, 2023. [Online]. Available: https://www.ije.ir/article_161610.html

[14] S. Thepade, S. Bang, P. Chaudhari, and M. Dindorkar, "Covid19 identification from chest x-ray images using machine learning classifiers with glcm features," *ELCVIA Electronic Letters on Computer Vision and Image Analysis*, vol. 19, p. 85, 11 2020.

[15] R. Saleh and H. Farsi, "Optimum ensemble classification for fully polarimetric sar data using global-local classification approach," *International Journal of Engineering*, vol. 31, no. 2, pp. 331–338, 2018. [Online]. Available: https://www.ije.ir/article_73125.html

[16] S. D. Thepade and A. R. Dhake, "Fusion of thepade sbtc and glcm features for recognizing gender from facial images," in *2021 Inter-*

national Conference on Communication information and Computing Technology (ICCICT), 2021, pp. 1–7.

[17] S. D. Thepade and S. S. Adrakatti, "Identification of aerial image land use using fused thepade sbtc and adaptive thresholding with machinelearning ensemble," in *2023 2nd International Conference for Innovation in Technology (INOCON)*, 2023, pp. 1–8.

[18] S. D. Thepade and A. P. Bhalerao, "Machine learning based land use identification of aerial images with fusion of thepade sbtc and triangle thresholding," in *2023 2nd International Conference for Innovation in Technology (INOCON)*, 2023, pp. 1–7.

[19] M. Madane and S. Thepade, "Score level fusion based bimodal biometric identification using thepade's sorted n-ary block truncation coding with variod proportions of iris and palmprint traits," *Procedia Computer Science*, vol. 79, pp. 466–473, 2016, proceedings of International Conference on Communication, Computing and Virtualization (ICCCV) 2016. [Online]. Available: https://www.sciencedirect.com/science/article/pii/S1877050916001915

[20] C. Eyupoglu, "Implementation of bernsen's locally adaptive binarization method for gray scale images," *The Online Journal of Science and Technology*, vol. 7, pp. 68–72, 04 2017.

[21] S. Khade, S. Gite, S. D. Thepade, B. Pradhan, and A. Alamri, "Detection of iris presentation attacks using feature fusion of thepade's sorted block truncation coding with gray-level co-occurrence matrix features," *Sensors*, vol. 21, no. 21, p. 7408, Nov 2021. [Online]. Available: http://dx.doi.org/10.3390/s21217408

[22] S. D. Thepade, R. Gaurav, and M. Shubham, "Hybrid wavelet transform based melanoma identification using ensemble of machine learning algorithms," *ELCVIA: electronic letters on computer vision and image analysis*, vol. 19, no. 3, pp. 1–17, Aug. 2020. [Online]. Available: https://raco.cat/index.php/ELCVIA/article/view/373196

Sudeep D Thepade Sudeep D Thepade is working as a Professor in Computer Engineering at Pimpri Chinchwad College of Engineering, Savitribai Phule Pune University, Pune, India. His current research interests include image classification, CBIR, image enhancements and biometric identification. He has more than 350 research papers to his credit. He has guided six Ph.D. Scholars and is currently guiding two PhD. Scholars and several Masters Dissertation Projects.

Ayush G Dudhani is a UG research scholar working with computer engineering at Pimpri Chinchwad College of Engineering. He is working on machine learning-based classification of histopathological images for effective feature formation. His areas of interest are machine learning and image processing.